

Nuclear-Magnetic-Resonance Properties of the Staircase Kagomé Antiferromagnet $\text{PbCu}_3\text{TeO}_7$

This content has been downloaded from IOPscience. Please scroll down to see the full text.

2015 Chinese Phys. Lett. 32 127503

(<http://iopscience.iop.org/0256-307X/32/12/127503>)

View [the table of contents for this issue](#), or go to the [journal homepage](#) for more

Download details:

IP Address: 159.226.35.181

This content was downloaded on 06/01/2016 at 10:10

Please note that [terms and conditions apply](#).

Nuclear-Magnetic-Resonance Properties of the Staircase Kagomé Antiferromagnet $\text{PbCu}_3\text{TeO}_7$ *

DAI Jia(代佳)¹, WANG Peng-Shuai(王朋帅)¹, SUN Shan-Shan(孙珊珊)¹, PANG Fei(庞斐)¹,
ZHANG Jin-Shan(张金珊)², DONG Xiao-Li(董晓莉)³, YUE Gen(乐艮)³, JIN Kui(金魁)³,
CONG Jun-Zhuang(丛君状)³, Sun Yang(孙阳)³, YU Wei-Qiang(于伟强)^{1**}

¹Department of Physics, Renmin University of China, Beijing 100872

²School of Energy, Power and Mechanical Engineering, North China Electric Power University, Beijing 102206

³Beijing National Laboratory for Condensed Matter Physics, Institute of Physics,
Chinese Academy of Sciences, Beijing 100190

(Received 25 July 2015)

We report the first nuclear magnetic resonance (NMR) study on single crystals of staircase Kagomé antiferromagnet $\text{PbCu}_3\text{TeO}_7$ ($T_{N1} \sim 36$ K). A Curie constant $\Theta \sim -140$ K is obtained by a Curie–Weiss fit to the high-temperature Knight shift of ^{125}Te . The hyperfine coupling constant is estimated to be $^{125}A_{\text{hf}} = -67$ kOe/ μ_B , and a strong interlayer coupling among staircase Kagomé planes is suggested with such a large hyperfine coupling, according to the lattice structure. The $^{63,65}\text{Cu}$ NMR spectra are found by the zero-field (ZF) NMR at $T = 2$ K, and the internal hyperfine fields are estimated to be 10.3 T and 9.6 T, for Cu(1) and Cu(2) sites, respectively, in the lattice. A second type of ZF NMR signal with a large rf enhancement is also seen after field-cycling through a high magnetic field.

PACS: 75.10.Jm, 76.60.-k

DOI: 10.1088/0256-307X/32/12/127503

The ground states and excitations of geometrically frustrated quantum magnets have attracted enormous interest in condensed matter physics. Particularly, two-dimensional $S=1/2$ Kagomé Heisenberg antiferromagnets may have novel quantum disordered states, such as spin liquids, due to strong quantum fluctuation and magnetic frustration.^[1–4] For systems with imperfect Kagomé structure, magnetic anisotropy induced by Dzyaloshinsky–Moriya interaction,^[5] spatial anisotropic exchange,^[6] and/or interlayer coupling may reduce geometry frustration and lead to antiferromagnetic ordering with very low Néel temperatures.

On the other hand, the interplay of geometric frustration, magnetic anisotropy, and quantum fluctuations produces competing ground states with complex magnetic structures, and also leads to potential multifunctional materials. A staircase Kagomé lattice with buckled Kagomé layers is one example, which has been realized in several materials such as $\text{A}_3\text{V}_2\text{O}_8$ ($\text{A}=\text{Cu}, \text{Co}, \text{Ni}$)^[7–9] and $\text{PbCu}_3\text{TeO}_7$.^[10] Consecutive magnetic transitions and magnetism induced ferroelectricity were reported in $\text{Ni}_3\text{V}_2\text{O}_8$, characterizing a multiferroic material with strong magnetoelectric coupling.^[11,12] The lattice structure of the newly discovered $\text{PbCu}_3\text{TeO}_7$ is illustrated in Fig. 1. The planes are stacked along the crystalline a direction with Pb and Te atoms as spacer layers. Each buckled Kagomé layer has two nonequivalent copper sites, Cu(1) in CuO_6 octahedrons and Cu(2) in CuO_4 tetrahedrons with a ratio of 2:1, each aligned in chains along the b direction. The magnetic couplings among neighboring Cu(1) spins, and neighboring Cu(1) and Cu(2) spins, are not uniform through corner and edge sharing oxygen,^[10] and therefore the system deviates from

an ideal Kagomé lattice antiferromagnet. It has been reported that the Weiss constant Θ obtained from the magnetic susceptibility is about -140 K, whereas consecutive antiferromagnetic transitions occur at much lower temperatures with $T_{N1} \sim 36$ K, $T_{N2} \sim 25$ K, and $T_{N3} \sim 17$ K, and their respective magnetic structures are still not yet resolved.^[10]

In this Letter, we present the first nuclear magnetic resonance (NMR) study on $\text{PbCu}_3\text{TeO}_7$, which is helpful for understanding its magnetic properties microscopically. Our high-temperature ^{125}Te Knight shift data in the paramagnetic phase reveals a large hyperfine coupling on the ^{125}Te sites. This suggests a strong interlayer hyperfine coupling, which should help the magnetic ordering of the system. Below the Néel temperature, the zero-field (ZF) NMR spectra are consistent with Cu signals from both the Cu(1) and Cu(2) sites. In addition, we also find a second ZF NMR signal, which has a large rf enhancement and is only detectable after field cycling through high magnetic fields. Here the field cycling refers to a process in which a finite magnetic field (H_{cycle}) is first switched on and then reduced to zero at the same temperature. We discuss that the second signal is likely to be from quenched disorder which is ferromagnetic in the frustrated magnet.

The $\text{PbCu}_3\text{TeO}_7$ single crystals were grown by the flux growth method with NaCl/KCl as flux.^[10] Our x-ray diffraction (data not shown) and susceptibility data (Fig. 2(b)) are consistent with the literature.^[10] The high-temperature bulk susceptibility was measured in a superconducting quantum interference device magnetometer, and the low-temperature magnetization was measured in a vibrating sample magne-

*Supported by the National Natural Science Foundation of China under Grant Nos 11374364 and 11222433, the National Basic Research Program of China under Grant No 2011CBA00112, and the Scientific Research Foundation for the Returned Overseas Chinese Scholars of State Education Ministry.

**Corresponding author. Email: wqyu_phy@ruc.edu.cn

© 2015 Chinese Physical Society and IOP Publishing Ltd

tometer. The NMR measurements were conducted on single crystals with mass ~ 3 mg, with a field applied along the crystalline [011] direction at the paramagnetic phase and under ZF in the ordered phase. The NMR spectra were collected by the standard spin-echo sequence. The high-temperature ^{125}Te spectra were obtained by fast Fourier transform of the spin-echo signal. The Knight shift in the paramagnetic phase was calculated with $^{125}K = f/^{125}\gamma H - 1$, where f is the central frequency of the resonance line, H is the external field, and $^{125}\gamma = 13.454 \text{ MHz/T}$ is the gyromagnetic ratio. The low-temperature broad ZF $^{63,65}\text{Cu}$ spectra were obtained by integrating the spin-echo intensity with frequency swept through the resonance line.

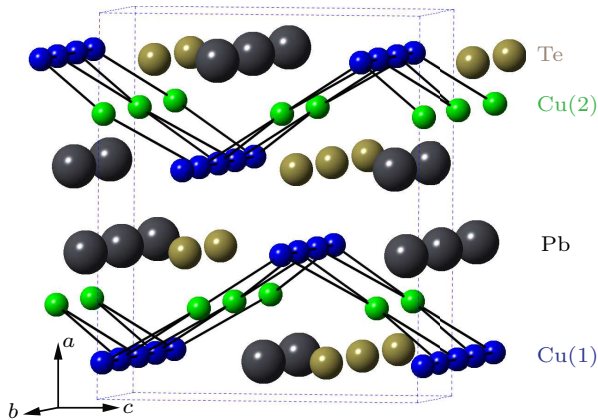


Fig. 1. (Color online) Crystal structure of $\text{PbCu}_3\text{TeO}_7$. Cu(1) in CuO_6 octahedrons and Cu(2) in CuO_4 tetrahedrons (oxygen not drawn) form the buckled Kagomé lattice layer. Te and Pb are spacers to separate the Kagomé layers.

The ^{125}Te ($I = 1/2$) NMR spectra, with temperatures from 275 K down to 37 K, are shown first in Fig. 2(a). Upon cooling, the spectra shift to lower frequencies and their full width at half maximum increase significantly ($\sim 40 \text{ kHz}$ at 275 K and $\sim 300 \text{ kHz}$ at 37 K). With the temperature down to 36 K, the NMR signal is too broad to be detectable, which is an indication of magnetic transition, consistent with T_{N1} detected by the susceptibility measurements.

The Knight shift ^{125}K is calculated and shown as a function of temperature in Fig. 2(b). Here ^{125}K is close to zero at 275 K and decreases with temperature as it cools, indicating a negative hyperfine coupling transferred from copper ions. The Knight shift above 100 K is well fit with a Curie-Weiss form, $^{125}K(T) = A + C/(T - \Theta)$, as shown by the dashed line in Fig. 2(b). The fitting gives $\Theta \sim -140 \pm 20 \text{ K}$, which is much higher than the Néel temperature, and therefore strong magnetic frustration is suggested.

In Fig. 2(b), we further plot our bulk susceptibility data χ of the crystal, measured as a function of temperature with a 1 T field. Here χ also shows a Curie-Weiss increase upon cooling, consistent with the reported data.^[10] In the inset of Fig. 2(b), ^{125}K is plotted against χ with temperature as an implicit parameter, where a linear relation between them is clearly seen. From the formula $^{125}K = \frac{^{125}A_{\text{hf}}}{N_A \mu_B} \chi$, where

μ_B is the Bore magneton and N_A is Avogadro's constant, the hyperfine coupling constant is calculated to be $^{125}A_{\text{hf}} = -67 \text{ kOe}/\mu_B$. Such a large hyperfine coupling indicates that the ^{125}Te is strongly coupled to the Cu moments. In principle, both dipolar interaction and exchange polarization mechanisms contribute to the $^{125}A_{\text{hf}}$. Given that Te atoms are in the interlayer sites, the dipolar interaction between the ^{125}Te nuclei and the Cu(1)/Cu(2) moments should be weak. On the other hand, theoretical studies predicted that a large negative A_{hf} can be obtained by an exchange polarization transfer mechanism from an empty d -orbital of the metal ions.^[13] For comparison, a large negative $^{125}A_{\text{hf}}$ has also been reported in $\text{Na}_2\text{Cu}_2\text{TeO}_6$ due to the hopping path Cu-O-Te-O-Cu.^[14] In the case of $\text{PbCu}_3\text{TeO}_7$, the strong interlayer hopping path containing Te atoms is consistent with electron structure calculation.^[10] Therefore, the large $^{125}A_{\text{hf}}$ should primarily originate from the participation of Te atoms through the hopping paths. Among all interlayer hopping paths, the strongest one is Cu(1)-O-Te-O-Cu(2), as shown by the dashed lines in the inset of Fig. 2(a), where two Cu atoms are from neighboring Kagomé planes. Given such a large hyperfine coupling observed on the ^{125}Te sites, our data suggests that the interlayer coupling is strong in this material. As a result, such a strong interlayer magnetic coupling should enhance the three-dimensional magnetic ordering with a high Néel temperature (36 K).

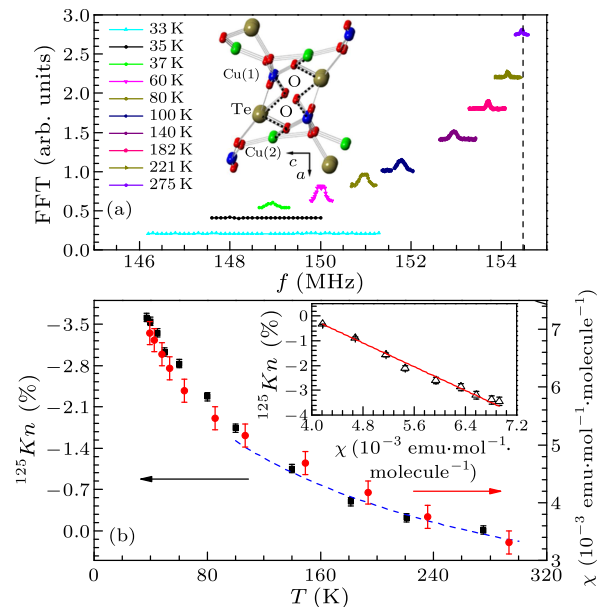


Fig. 2. (Color online) (a) High-temperature NMR spectra of ^{125}Te with a fixed field $\mu_0 H = 11.5 \text{ T}$, applied along the crystalline [011] direction. The vertical dashed line denotes the reference frequency at zero Knight shift. Inset: the major interlayer hopping path Cu(1)-O-Te-O-Cu(2) denoted by the dashed line. (b) The temperature dependence of the Knight shift $^{125}K_n$ (squares) and the bulk susceptibility χ (circles). The blue dashed line is the fit of the $^{125}K_n$ to the function $^{125}K(T) = A + C/(T - \Theta)$ above 100 K. Inset: $^{125}K_n$ plotted against magnetic susceptibility χ above T_{N1} , where the straight line is a linear fit to the data.

We have not found the $^{63,65}\text{Cu}$ NMR signal spec-

tra in the paramagnetic state, possibly due to the strong magnetic fluctuations on the Cu sites. However, at temperatures far below the Néel transition, a ZF NMR spectrum is obtained from 65 MHz to 145 MHz at $T = 2$ K, after ZF cooling. The spectrum is marked as A1 to distinguish from the second NMR signal (A2) which we will describe in the following. The observation of the ZF spectrum indicates the internal hyperfine fields due to magnetic ordering. The A1 spectra have been checked by NMR measurements on several crystals, and their lineshapes are consistent.

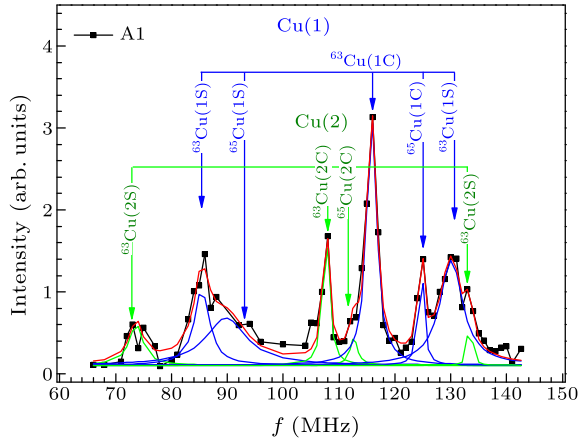


Fig. 3. (Color online) The ZF Cu spectrum measured at 2 K with a normal rf excitation power (A1, solid squares). The blue and green arrows denote the signal from the Cu(1) and Cu(2) sites, respectively. The subscript c represents the central lines and s the satellite lines.

The NMR spectrum is very broad, with a finite background and six peak-like features from 65 MHz to 140 MHz. With such a large resonance frequency and the multiple peak feature, we can conclude that the signal is impossible from ^{125}Te , which is a spin-1/2 nuclei. On the other hand, considering Cu(1) and Cu(2) sites in this staircase Kagomé lattice, and two types of spin-3/2 copper nuclear isotopes (^{63}Cu and ^{65}Cu), twelve Cu NMR lines are expected with four center transitions and eight satellite transitions. Therefore, it is reasonable to attribute the observed NMR spectrum from Cu isotopes. In particular, we assign the narrow lines to the center transitions which have weak second order quadrupolar corrections, compared with the satellite lines with the first order corrections, due to lattice inhomogeneity. Given the gyromagnetic ratio of $^{63}\gamma = 11.285$ MHz/T and $^{65}\gamma = 12.099$ MHz/T, and the natural abundance of 69% and 31% for ^{63}Cu and ^{65}Cu respectively, we first tentatively associate the observed narrow NMR peaks to four center transitions as shown by the arrows labeled with $^{63}\text{Cu}(1c)$, $^{65}\text{Cu}(1c)$, $^{63}\text{Cu}(2c)$, and $^{65}\text{Cu}(2c)$, respectively. This is roughly consistent with the theoretical value of the relative spectral weight $^{63}\text{Cu}(1c):^{65}\text{Cu}(1c):^{63}\text{Cu}(2c):^{65}\text{Cu}(2c) \approx 128:62:69:31$, and the relative hyperfine fields on Cu(1) and Cu(2) sites. However, we have difficulty resolving all satellite lines. Nevertheless, we attempt to assign several peaks to the satellite transition as labeled in Fig. 3, given the quadrupole moments of 0.211 and 0.195

barns for ^{63}Cu and ^{65}Cu , respectively.

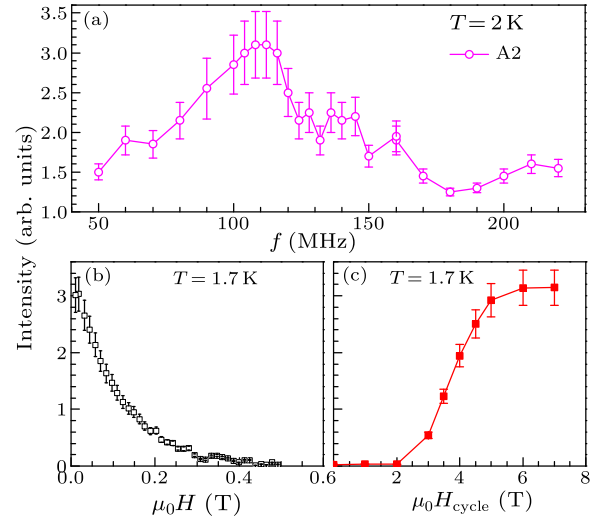


Fig. 4. (Color online) (a) The zero-field spectra measured at 2 K with a low rf power and after a 6 T field cycling (A2, open circles). The vertical scale is the same as Fig. 3. (b) The echo intensity of A2 after a 6 T field cycling, as a function of measurement field with fixed resonance frequency $f = 116$ MHz. (c) The echo intensity of A2 as a function of the cycling field H_{cycle} with fixed $f = 116$ MHz and with zero measurement field.

The internal hyperfine fields on Cu(1) and Cu(2) sites are estimated to be $B_{\text{in}}(1) \sim 10.3$ T and $B_{\text{in}}(2) \sim 9.6$ T, respectively. Here we neglect the second-order quadrupolar correction to the center lines, which is in an order of 2 MHz estimated from the line splitting of the satellites. We note that the A1 spectrum does not show hysteresis with temperature or field changes, and no obvious rf enhancement is observed in comparison with the ^{125}Te NMR in the paramagnetic phase, as expected for the bulk NMR signal in the ordered antiferromagnetic phase.

In the following, we show a second ZF NMR signal with a large rf enhancement, which is created at low temperatures after field cycling through a high magnetic field. When lowering the excitation power, the A1 signal is completely suppressed, and another ZF signal in the same frequency range appears. As shown in Fig. 4(a), the ZF spectrum at $T = 2$ K, labeled as A2, is obtained after field cycling under a 6 T field, and the optimized rf excitation power is 22 dB lower than that of the A1 spectra under the same pulse length. Therefore, an rf enhancement factor $\eta \sim 20$ is estimated for the A2 signal. Here the same vertical scale is used for Figs. 3 and 4(a) for comparison.

The A2 signal is not seen after ZF cooling from high temperatures, whereas A1 does not change under different fields or thermal treatments. The hysteresis of the A2 spectrum is further measured under a magnetic field H and with different cycling fields H_{cycle} . As shown in Fig. 4(b), after field cycling under a 6 T field, the measurement is taken under an external magnetic field H from 0 to 0.4 T, the echo intensity at 116 MHz (center of the spectrum) is quickly suppressed to zero. In Fig. 4(c), the echo intensity is shown as a function of the cycling field H_{cycle} , while

the external measurement field remains zero. The echo intensity is zero with the H_{cycle} from 0 to 2 T, then it starts to increase rapidly with the H_{cycle} from 3 T to 6 T, and saturates with the H_{cycle} above 6 T. Clearly, the signal strength is enhanced after field cycling through a threshold field (3 T), while is suppressed under a small external measurement field.

Compared with A1, A2 is broadly distributed above 140 MHz and peaks at ~ 115 MHz, and the signal intensities for A1 and A2 have the same magnitude. Considering that A2 exists in a similar frequency range as signal A1, we attribute the A2 signal to $^{63/65}\text{Cu}$ NMR as well. The spin-spin relaxation time T_2 is about $14 \mu\text{s}$ for A2 at 2 K, much shorter than that of A1 with $T_2 \sim 60 \mu\text{s}$ (data not shown). Strong magnetic fluctuation is suggested for the A2 spectrum. Therefore, A2 is characterized by nuclei environments with strong thermal and field hysteresis, a large rf enhancement, strong magnetic fluctuations, and inhomogeneous hyperfine fields. Since NMR is a local probe, the differences in the field hysteresis and in T_2 between A1 and A2 suggest different regions of the sample.

It is known that ZF NMR in ordered ferromagnets has large rf enhancement, fast relaxation, and broad linewidth due to domain wall dynamics, and the signal intensity is suppressed under magnetic fields.^[15] Our A2 signal is consistent with the NMR signal from ferromagnet domains, although bulk $\text{PbCu}_3\text{TeO}_7$ is an antiferromagnet. In fact, we show that the A2 signal does not represent bulk properties of the sample. First, if we normalize the NMR intensity by the rf enhancement factor, the intensity of the A2 signal at 116 MHz is about 5% of A1. Secondly, the magnetization data measured at 2.2 K, as shown in Fig. 5, increases linearly with the field from 0 T to 12 T. Therefore, no evidence for field induced spin flop or other magnetic transitions in the bulk sample accounts for the field cycling induced NMR signal.

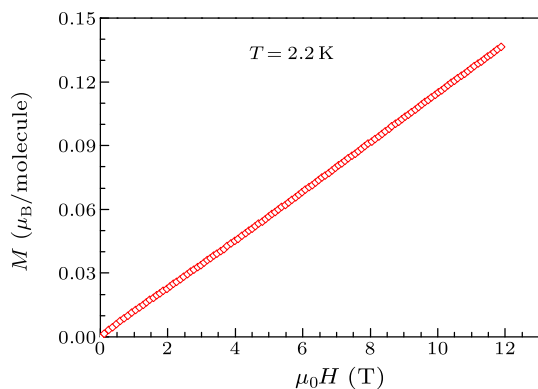


Fig. 5. The magnetization curve measured at 2.2 K with a field from 0 up to 12 T applied along the [011] crystalline direction.

In fact, our A2 signal is consistent with the quenched disorder in a frustrated antiferromagnet. In the frustrated system, the ground states are highly

degenerate,^[16–18] and the net ferromagnetic moment may be created close to quenched disorder. In this case, an external field above a threshold field polarizes the defects and their neighboring spins, and therefore creates small ferromagnetic domains surrounding the defects in the antiferromagnetic background. When the cycling field is removed, the remnant ferromagnetism leads to a large ZF NMR signal. Since the domain size is small, the NMR signal from this region should have a short T_2 and a large rf enhancement as seen in a regular ferromagnet. We indeed observed similar field cycling induced NMR signals in other frustrated magnets, including CuBr_2 and FeVO_4 (data not shown). Therefore, the field cycling induced NMR signal is likely a characteristic feature for a frustrated magnet with a quenched disorder.

We note that the field cycling induced NMR signal has been reported in a spin glass system Cu–Mn alloy^[19] and a frustrated antiferromagnet TbMn_2O_5 .^[20] In the case of the Cu–Mn alloy, field cycling induces remnant magnetization and results in an enhanced bulk NMR signal from coherence of neighboring spins.^[19] For TbMn_2O_5 , the enhanced NMR signal is attributed to the field cycling induced ferromagnetic ordering of Tb moments.^[20] These observations, included in our case, are consistent with the fact that remnant ferromagnetism plays an essential role for the induced NMR signal.

In summary, we have investigated the magnetic properties of the frustrated staircase Kagomé compound $\text{PbCu}_3\text{TeO}_7$ by NMR. Strong interlayer coupling is suggested by the large ^{125}Te Knight shift in the paramagnetic phase. We also identify the hyperfine fields on Cu(1) and Cu(2) sites, which gives microscopic information for the magnetic structure. A second type NMR signal is also seen by a field cycling process, which may be a characteristic feature for a frustrated magnet with a quenched disorder.

References

- [1] Sachdev S 1992 *Phys. Rev. B* **45** 12377
- [2] Lecheminant P et al 1997 *Phys. Rev. B* **56** 2521
- [3] Yan S et al 2011 *Science* **332** 1173
- [4] Depenbrock S et al 2012 *Phys. Rev. Lett.* **109** 067201
- [5] Cépas O et al 2008 *Phys. Rev. B* **78** 140405
- [6] Schnyder A P et al 2008 *Phys. Rev. B* **78** 174420
- [7] Shannon R D and Calvo C 1972 *Can. J. Chem.* **50** 3944
- [8] Fuess H et al 1970 *Acta Crystallogr. B* **26** 2036
- [9] Sauerbrei E E et al 1973 *Acta Crystallogr. B* **29** 2304
- [10] Koteswararao B et al 2013 *J. Phys.: Condens. Matter* **25** 336003
- [11] Lawes G et al 2004 *Phys. Rev. Lett.* **93** 247201
- [12] Lawes G et al 2005 *Phys. Rev. Lett.* **95** 087205
- [13] Owen J and Thornley J H M 1966 *Rep. Prog. Phys.* **29** 675
- [14] Morimoto K et al 2006 *J. Phys. Soc. Jpn.* **75** 083709
- [15] Turov E A and Petrov M P 1972 *Nuclear Magnetic Resonance in Ferro- and Antiferromagnets* (New York: Israel Program of Scientific Translations)
- [16] Heid C et al 1995 *J. Magn. Magn. Mater.* **151** 123
- [17] Chen Y et al 2006 *Phys. Rev. B* **74** 014430
- [18] Lorenz B et al 2004 *Phys. Rev. Lett.* **92** 087204
- [19] Alloul H 1979 *Phys. Rev. Lett.* **42** 603
- [20] Baek S H et al 2006 *Phys. Rev. B* **74** 140410(R)